Thesis for the degree of Licentiate of Engineering

Aviation climate impact and opportunities for mitigation

Filip Herbertsson

Department of Mechanical Engineering
CHALMERS UNIVERSITY OF TECHNOLOGY
Göteborg, Sweden 2026

Aviation climate impact and opportunities for mitigation
FILIP HERBERTSSON

Licentiatavhandlingar vid Chalmers tekniska högskola

Department of Mechanical Engineering
Chalmers University of Technology
SE–412 96 Göteborg, Sweden
Telephone + 46 (0) 31 – 772 1000

Chalmers Reproservice
Göteborg, Sweden 2026

"...the truth, to which only a brief triumph is allotted between the two long periods in which it is condemned as paradoxical or disparaged as trivial."

— Arthur Schopenhauer

Abstract

Aviation climate impact and opportunities for mitigation
FILIP HERBERTSSON
Department of Mechanical Engineering
Division of Fluid Dynamics
Chalmers University of Technology

Climate impact from aviation is an ever-growing concern, driven by the continued increase in air traffic and associated emissions. The climate impact extends beyond carbon dioxide (CO_2), with non-CO_2 emissions and contrail formation together constituting a substantial share of the sector's total anthropogenic radiative forcing. This thesis develops methods to evaluate the different contributions to aviation-induced climate impact, with particular emphasis on non-CO_2 effects. It then describes the metrics used to compare emissions with fundamentally different characteristics. Mitigation pathways aimed at reducing aviation's overall climate footprint are evaluated. Special focus is placed on contrails, which represent a highly variable but potentially dominant component of aviation's climate impact and offer opportunities for mitigation through targeted operational measures. The climate impact of Swedish aviation is assessed and attributed to individual emission species, highlighting the significant contribution of non-CO_2 effects and the strong spatial, temporal, and seasonal variability of contrail formation. The results indicate that a relatively small subset of flights is responsible for a disproportionate share of contrail-induced warming, suggesting that selective contrail avoidance strategies could yield substantial climate benefits with limited operational disruption and cost. In addition to operational measures, this thesis investigates technological solutions, with a detailed analysis of the Water Enhanced Turbofan (WET) engine concept, which has been proposed as a means to reduce fuel burn as well as emissions of nitrogen oxides (NO_x) and contrails. The performance and thermodynamic constraints of the WET engine are evaluated, showing that installation effects may offset its previously predicted advantages. Overall, the findings in this thesis underscore the importance of addressing non-CO_2 effects in aviation climate assessments and demonstrate that both targeted operational strategies and careful evaluation of emerging technologies are essential for achieving meaningful reductions in the sector's climate impact.

Keywords: climate impact, non-CO_2 effects, contrail avoidance, fuel burn, Water Enhanced Turbofan, steam injection, sustainable aviation

Författarens tack

Det här har varit det svåraste kapitlet att skriva eftersom så många på olika sätt har bidragit till avhandlingen och förtjänar ett tack. Jag hoppas att ingen känner sig bortglömd.

Jag vill börja med att tacka min handledare Tomas som gjort projektet möjligt och som har väglett mig genom alla utmaningar. Du har ett fantastiskt ärligt sätt att uttrycka dig på och våra möten är sällan tråkiga. Tack för att du trodde på mig redan under min grundutbildning och för den frihet du har gett mig i mitt arbete.

Jag vill också tacka Turboroomet+ för att ni orkar lyssna när jag i detalj beskriver mina buggar, för att ni delar era framgångar och bakslag med mig, och för att ni lyckas få en 8-timmars arbetsdag att kännas som en enda lång fikarast. Även om den ibland också blir just det. Det är ni som ger mening åt att gå till kontoret varje dag. Tack också till alla andra kollegor, informella handledare och tekniska gurus som delar med sig av sin visdom.

Ett stort tack till mina vänner i Kanelbullechatten som drar bort mig från jobbet och får mig att tänka på annat en stund. Tack till min familj för att ni tror på mig och stöttar mig, även när ni inte förstår vad jag gör eller varför jag gör det.

Slutligen vill jag tacka min fästmö Elin, kärleken i mitt liv som alltid står vid min sida, och som heroiskt höll ordning hemma medan jag skrev avhandlingen utan att klaga (åtminstone inte högt). En shoutout också till min katt Bosse som har varit väldigt förstående under den här tuffa perioden.

Filip Herbertsson
Göteborg, April 2026

List of Publications

This thesis is based on the following appended papers:

Manuscript 1. Filip Herbertsson, Xin Zhao, Anders Lundbladh, Tomas Grönstedt. *Performance assessment of the Water Enhanced Turbofan engine.* Aerospace Science and Technology. Nov 2026, p. 112389. DOI: 10.1115/1.4065922

Manuscript 2. (Submitted manuscript) Filip Herbertsson, Tomas Grönstedt. *Quantifying Aviation's Non-CO_2 Climate Impact in the Nordic Environment.* AIAA Aviation Forum 2026. Jun 2026. San Diego, California, USA

Nomenclature

Acronyms

ACI	–	Aerosol-Cloud Interaction
AR	–	Aspect Ratio
ARI	–	Aerosol-Radiation Interaction
ATR	–	Average Temperature Response
BADA	–	Base of Aircraft Data
BAU	–	Business As Usual
BFFM2	–	Boeing Fuel Flow Method
BPR	–	Bypass Ratio
CO_2	–	Carbon Dioxide
CoCiP	–	Contrail Cirrus Prediction model
EF	–	Energy Forcing
EGWP	–	Effective Global Warming Potential
ERF	–	Effective Radiative Forcing
FaIR	–	Finite Amplitude Impulse Response model
FAR	–	Fuel-Air Ratio
FPR	–	Fan Pressure Ratio
GGP	–	Generalized Geometric Parameters
GTP	–	Global Temperature change Potential
GWP	–	Global Warming Potential
IRF	–	Instantaneous Radiative Forcing
ISSR	–	Ice-Supersaturated Region
LHV	–	Lower Heating Value
LMTD	–	Logarithmic Mean Temperature Difference
LTO	–	Landing and Take-Off
MEEM2	–	nvPM Mission Emissions Estimation Methodology
NO_x	–	Nitrogen Oxides
nvPM	–	Non-volatile Particulate Matter
OEM	–	Original Equipment Manufacturer
RF	–	Radiative Forcing
RPK	–	Revenue Passenger Kilometer
SAF	–	Sustainable Aviation Fuels
SR	–	Specific Range
SWV	–	Stratospheric Water Vapor

TIT	–	Turbine Inlet Temperature
TSFC	–	Thrust Specific Fuel Consumption
vPM	–	Volatile Particulate Matter
WAR	–	Water-Air Ratio
WET	–	Water Enhanced Turbofan

Latin Letters

A	–	surface area of earth [m^2]
c	–	velocity [m/s]
C	–	coefficient [–]
d	–	diameter [m]
D	–	drag [N]
F	–	thrust [N]
H	–	time horizon [yr]
K	–	shape constant [–]
l	–	length [m]
L	–	lift [N]
$\dot{m}$	–	mass flow rate [kg/s]
p	–	pressure [Pa]
$\dot{Q}$	–	heat transfer rate [W]
r	–	efficacy [–]
S	–	area [m^2]
t	–	time [yr]
T	–	temperature [K]
U	–	heat transfer coefficient [$W/(m^2\,K)$]
w	–	weight [N]
$\dot{W}$	–	power [W]
X	–	specie [–]

Greek Symbols

α	–	surface-area-density [1/m]
γ	–	ratio of specific heats [–]
η	–	efficiency [–]
σ	–	void-fraction [–]
τ	–	lifetime [yr]
χ	–	compactness fraction [–]
Ω	–	rotational speed [rad/s]

Subscripts

0	–	freestream
01	–	total property at inlet
02	–	total property at outlet
9	–	nozzle exit
A	–	end A
AC	–	aircraft
B	–	end B
eng	–	engine
fuse	–	fuselage
kin	–	kinetic
f	–	fuel
nac	–	nacelle
o	–	overall
p	–	polytropic
pl	–	payload
pr	–	propulsive
r	–	ratio
ref	–	reference
th	–	thermal
wet	–	wetted
wing	–	wing

Contents

Part I

Introductory Chapters

Chapter 1

Introduction

1.1 Aviation and climate

Aviation has been estimated to produce emissions that account for 100.9 mW/m^2 of anthropogenic effective radiative forcing (ERF) in 2005 [2]. This corresponds to 3.5 % of the global anthropogenic ERF, increasing to 4.9 % when aircraft-induced cirrus clouds are included. ERF measures the additional heat radiation added to the Earth's climate system. For a detailed definition of this and other climate metrics, see Section 1.3.

The sector is improving in efficiency. Between 1940 and 2014 the fuel consumption per revenue passenger kilometer (RPK) decreased by an average of 1.3 % per year [3], reducing carbon dioxide (CO_2) emissions. However, despite significant efficiency improvements, total emissions continue to rise due to increased demand. Before the COVID-19 pandemic, Airbus and Boeing expected an annual increase of 4.4 % [4] and 4.6 % [5] in RPK respectively, both estimates outpacing the historical reduction in

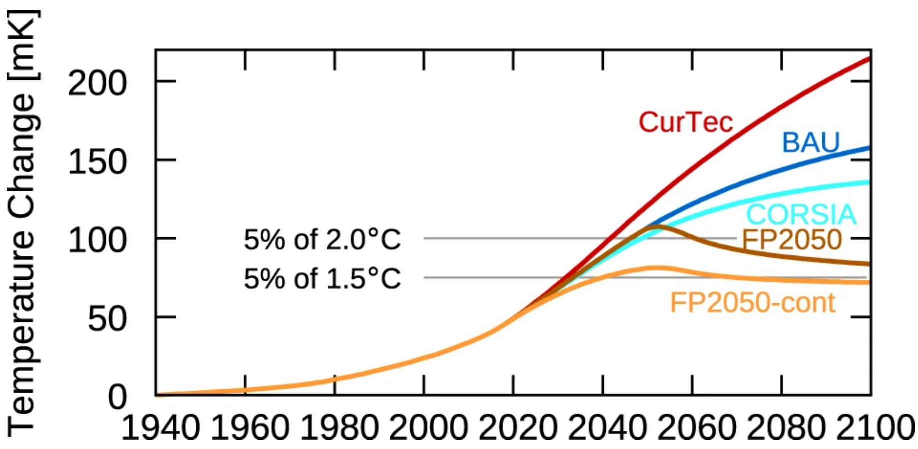

Figure 1.1: Temperature trajectories for different emission scenarios. CurTec refers to a continuation of the current generation aircraft. BAU refers to a business-as-usual case, where new engines and aircraft come out as frequently as before and with the same improvements. CORSIA refers to engines matching the CORSIA emissions reduction program. FP2050 and FP2050-cont. refers to emissions fulfilling the goals of the ACARE Flightpath 2050. Created by Grewe et al. (2021) [1].

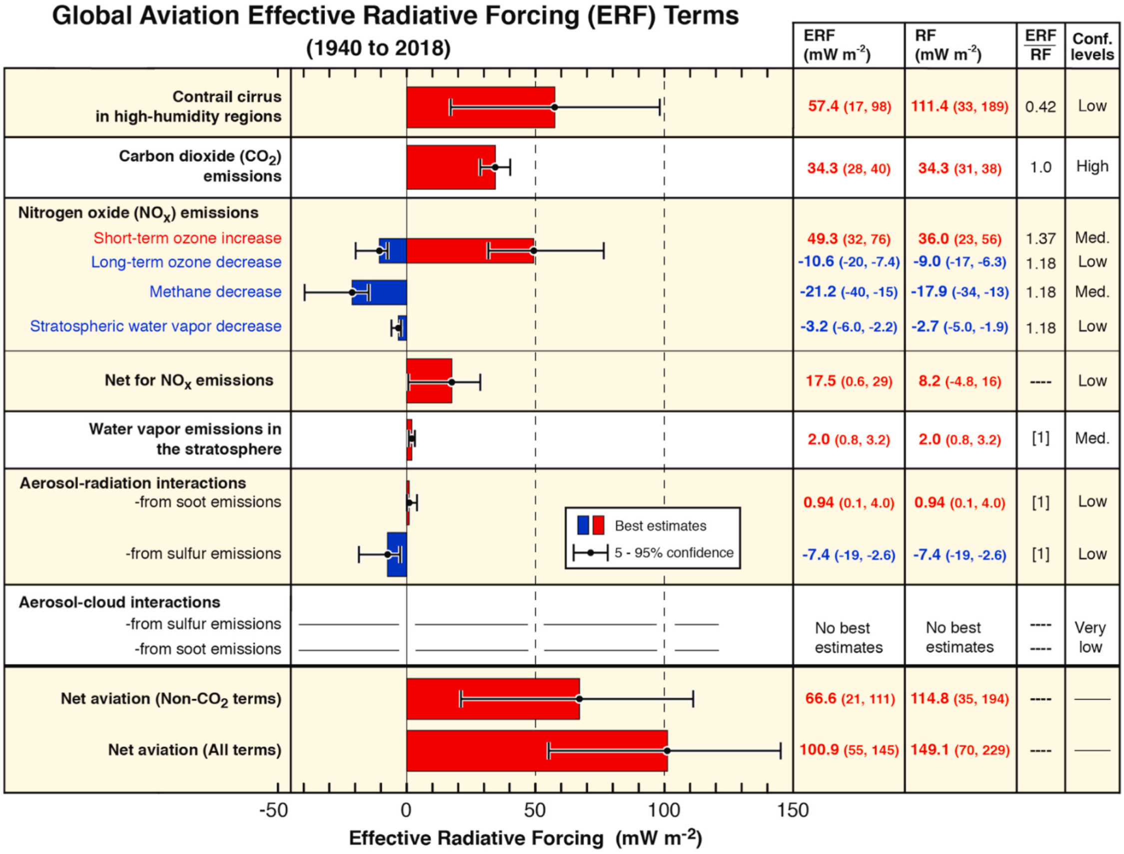

Figure 1.2: Climate impact from aviation emissions, measured in radiative forcing (RF) and effective radiative forcing (ERF). Reproduced from Lee et al. 2021 [6].

fuel consumption. During the COVID-19 pandemic, a temporary ban on international travel caused a significant reduction in air travel. However, most estimates show that the sector is now back to the levels before the pandemic and are growing.

Figure 1.1, produced by Grewe et al., shows the temperature increase from a pre-industrial state due to aviation up until 2020, and the expected future trajectory for five different scenarios. It is clear that with the current technology and with a business-as-usual approach, the global temperature change will continue to increase well beyond the year 2100 [1]. However, even the currently implemented emissions reduction program CORSIA fails to limit the maximum temperature change to the 2 °C set out by the Paris accords. Only more drastic emission scenarios, such as the goals set out by ACARE in their Flightpath 2050, where CO_2 per RPK is reduced by 75 % and nitrogen oxide (NO_x) emissions per RPK are reduced by 90 %, manages to live up to the Paris accords. This exemplifies the great challenge that the aviation sector faces in becoming environmentally friendly.

1.2 Non-CO_2 effects

The continuing increase in CO_2 emissions is problematic in itself. However, the largest climate impact comes from other emissions, colloquially known as non-CO_2

effects. Current research suggests that the total warming from aviation emissions, including non-CO_2 effects, is roughly three times as large as the warming from CO_2 alone. The main non-CO_2 effects include contrails and contrail-induced cirrus, NO_x, stratospheric water vapor (SWV), and aerosols. A comparison between the major aviation emissions by Lee et al. can be seen in Figure 1.2.

While CO_2 emissions depend only on fuel burn, non-CO_2 effects also depend on a range of other factors such as the design of the combustion chamber, cycle parameter selection, and ambient temperature and humidity. This complicates the issue of reducing aviation climate impact, and is both a blessing and a curse. On one hand, it is not enough to simply decarbonize aviation to remove the climate impact. Addressing climate change requires a multi-faceted approach in which the entire chain, from propulsion technology to aircraft operations, is adapted. On the other hand, non-CO_2 effects open up new avenues for climate impact mitigation that can be both quicker and have a larger impact than decarbonization.

1.2.1 Contrails

The largest non-CO_2 effects are contrails and contrail-induced cirrus clouds. They are estimated to have an ERF that is 67% larger than that of CO_2 emissions [6], although the uncertainty in these estimates remain high. Contrails, short for condensation trails, are water droplets from the exhaust of aircraft engines that freeze and form a white trail. Contrails can be persistent or non-persistent depending on whether the contrail remains in the atmosphere or gets absorbed shortly after it is formed. Persistent contrails have a large climate impact, whereas non-persistent contrails have a negligible climate impact. Persistent contrails can spread out and evolve into cirrus clouds, covering large areas and persisting for up to two days.

Contrails can cause both warming and a cooling effects depending on the time of day they form and the specific weather conditions. During the day, two effects are present. On the one hand, radiation from the sun is reflected out into space, causing a cooling effect. On the other hand, thermal radiation from the Earth's surface is reflected back toward the Earth, causing a warming effect. Which effect is stronger depends heavily on the specific contrail characteristics. During the night, however, there is no sunlight and thus only the warming effect remains. A more detailed discussion of the formation and climate impact of contrails can be found in Sections 2.1 and 2.2 as well as in Paper 2.

1.2.2 NO_x

Combustion in air at high temperatures and pressures inevitably causes the formation of NO_x, as nitrogen in the air is oxidized. The higher the temperature and pressure during the combustion, the more NO_x is produced. Historically, engine design research has gone towards increasing both the temperature and the pressure in the combustion chamber as this increases the thermal efficiency of the engine, reducing fuel consumption and CO_2 emissions. It is worth noting that it is not the average combustion temperature that is important for NO_x formation. Rather, it is the temperature reached in local hot-spots that causes the most emissions. This has led to the development of combustor technologies such as lean-burn, where the combustion happens at a much lower fuel-air ratio (FAR), which leads to lower combustion temperatures and less NO_x formation. As the awareness of the adverse effects of NO_x has increased, legislation on NO_x emissions through the ICAO CAEP/8 environmental standard forces the research focus towards limiting and reducing the NO_x emissions as well.

NO_x does not have a significant radiative forcing itself; rather, the major contribution to global warming from NO_x comes from its interaction with other greenhouse gases. NO_x increases the efficiency of ozone production, immediately causing more ozone and increased radiative forcing. In the long term, NO_x reduces the lifetime of methane, which has a cooling effect on the climate. The reduced methane concentration also leads to lower ozone in the long term, which contributes to the cooling effect. Lastly, NO_x leads to lower levels of SWV due to the reduced methane concentration, which also has a cooling effect. This is described more in-depth in Section 1.2.3. In total, there is a clear net warming effect from aviation NO_x emissions. However, the strengths of the warming and cooling components vary with altitude and at ground altitude the net climate impact is more uncertain.

1.2.3 Stratospheric water vapor

The atmosphere is divided into layers based on composition and dynamics. The lowest layers are called the troposphere, which is the part where the biosphere is, and the stratosphere, which is just above the troposphere and begins around typical aircraft cruise altitudes. The two layers are delimited by the tropopause. The stratosphere is an extremely dry region of the atmosphere and water in this region, SWV, tends to remain in the atmosphere for long periods of time. Affecting the water concentration in this region thus has an outsized climate impact compared to emission at ground level or in the troposphere. The tropopause is also not static; it differs with location and time and is highly correlated to the latitude and the day-of-year. At low latitudes near the equator the tropopause can reach altitudes as high as 17 km, while at high latitudes near the poles it can go below 8 km.

Water forms during combustion with jet fuel and when the aircraft is flying above the tropopause this water is released directly into the stratosphere, increasing the radiative forcing. However, the biggest impact from aviation on SWV comes from the NO_x emissions. One major natural pathway of forming SWV is through the oxidation of methane within the stratosphere. As NO_x emissions reduce the concentration of methane, less methane disperses to the stratosphere and so a net reduction in stratospheric methane oxidation is seen, causing lower levels of SWV and thus an apparent cooling effect. This effect is typically stronger than the warming effect of direct injection of water.

1.2.4 Soot, sulfate, and other aerosol particles

Aerosols are particles suspended in the atmosphere. The main aerosols from aviation are soot, sulfate and lubrication oil. Their impact on the climate can lead to both a warming and a cooling effect, depending on the particle material characteristics, shape and chemistry with the surrounding atmosphere. Soot, also known as non-volatile particulate matter (nvPM), is formed in the combustion chamber due to incomplete combustion. It is most prevalent when an engine is operating in a regime where high thrust output is required as this often leads to a high FAR near stoichiometric conditions. As the reactants are not perfectly mixed, spots are formed with lower oxygen content leading to incomplete combustion. Modern technologies, such as lean combustion, have lowered soot emissions substantially. Sulfates on the other hand are formed when sulfur is present in the fuel. Aviation fuel always contains some amount of sulfur due to its presence in the feedstock for fuel production. Recent efforts aim to limit the amount of sulfur allowed in jet fuel to reduce the formation of sulfates, which requires post-treatment of the fuel. Sulfate, lubrication oil and other volatile compounds are colloquially known as volatile particulate matter (vPM).

Aerosols impact the climate via two main pathways, aerosol-radiation interactions (ARI) and aerosol-cloud interactions (ACI). Via the ARI mechanism, the particles can either absorb or scatter incoming radiation. If the particles absorb incoming radiation, it leads to heating of the atmosphere and by extension heating of the climate. If the particles scatter incoming radiation, the climate impact depends on the type and extent of the radiation affected. Scattering of visible and ultra-violet light implies backscattering of sunlight, keeping it from interacting with the ground leading to a cooling effect. Scattering of infrared radiation leads to heat being trapped between the ground and the atmosphere, working as a metaphorical blanket, thus leading to a heating effect. Via the ACI mechanism, aerosols impact the formation, duration and radiative properties of natural clouds. Particles in the air act as nucleation sites for water droplets, causing clouds consisting of more ice particles where each particle is smaller in size. In general, ACI has a cooling effect on the climate, although it is much more difficult to estimate than ARI.

1.3 Climate impact and metrics

To measure and compare the impact of different climate forcers, multiple metrics can be used depending on the property of interest. The most basic metric is radiative forcing (RF), which describes how much additional power is received per unit surface area of the Earth due to an emission. RF changes over time, but if the interest is purely in the radiative forcing at the time of emission, instantaneous radiative forcing (IRF) can be used, which is defined as

$$\mathrm{IRF} = \mathrm{RF}(0). \tag{1.1}$$

Some climate forcers, such as CO_2, primarily cause increased energy uptake in the atmosphere by themselves. Other climate forcers, such as contrails, also affect the balance of natural systems, such as clouds. When contrails form, the can alter the formation and radiative effect of natural clouds, which reduces their net warming impact. To account for this, effective radiative forcing (ERF) can be used. While RF represents the change in radiation due to the emission itself, ERF represents the net change in radiation after the atmosphere has adjusted to the emission. The ratio of these is called efficacy, denoted r.

$$\mathrm{ERF}(t) = r\,\mathrm{RF}(t) \tag{1.2}$$

For contrails, the efficacy is estimated at around 0.42 [6]. This means that, on average, contrails causing $100\,\mathrm{mW/m^2}$ only result in a net forcing increase of $42\,\mathrm{mW/m^2}$, as they also offset forcing from natural clouds of $58\,\mathrm{mW/m^2}$. To get the total energy added to the Earth, referred to as energy forcing (EF), ERF is integrated over the lifetime of the emission, τ, and multiplied by the total surface area of the Earth (A).

$$\mathrm{EF} = A \int_0^{\tau} \mathrm{ERF}(t)\,dt. \tag{1.3}$$

When comparing two climate forcers, the most common metric is the global warming potential (GWP). This is defined as the integrated RF over a specific time horizon for a one kilogram emission, normalized by the integrated RF over the same time horizon for a one kilogram emission of CO_2. For emission X and time horizon H, we write it as

$$\mathrm{GWP}_H = \frac{\int_0^H \mathrm{RF}_X(t)\,dt}{\int_0^H \mathrm{RF}_{\mathrm{CO_2}}(t)\,dt}. \tag{1.4}$$

The numerator is known as the absolute global warming potential (AGWP). Typical time horizons for GWP are 20, 50, and 100 years, and the choice depends on whether short-term or long-term effects are of interest. Oftentimes all three are presented together to provide a clearer picture of the relative impacts. The effective global warming potential (EGWP) is similar to the GWP, but using ERF instead of RF. For aviation, it is more relevant to compare the energy forcing from actual emissions rather than from a one kilogram emission. Some emissions, primarily contrails, also do not have a well-defined mass that can be used for comparison. Therefore, in aviation, it is more common to compare the energy forcing caused by the actual amount of emissions, expressed in CO_2 equivalents.

For climate impact, global temperature change is the most relevant effect. However, the global mean temperature does not respond linearly to EF. The intensity profile and duration of the additional radiation matter, as does the expected release of other emissions. To get more meaningful metrics for the temperature response of the climate, the calculated ERF can be coupled with a climate model. One common metric is the global temperature change potential (GTP), which represents the global mean temperature response at a given time following a one kilogram emission. Another metric is the average temperature response (ATR), which is defined as

$$\mathrm{ATR} = \frac{1}{H} \int_0^H \mathrm{GTP}(t)\,dt. \tag{1.5}$$

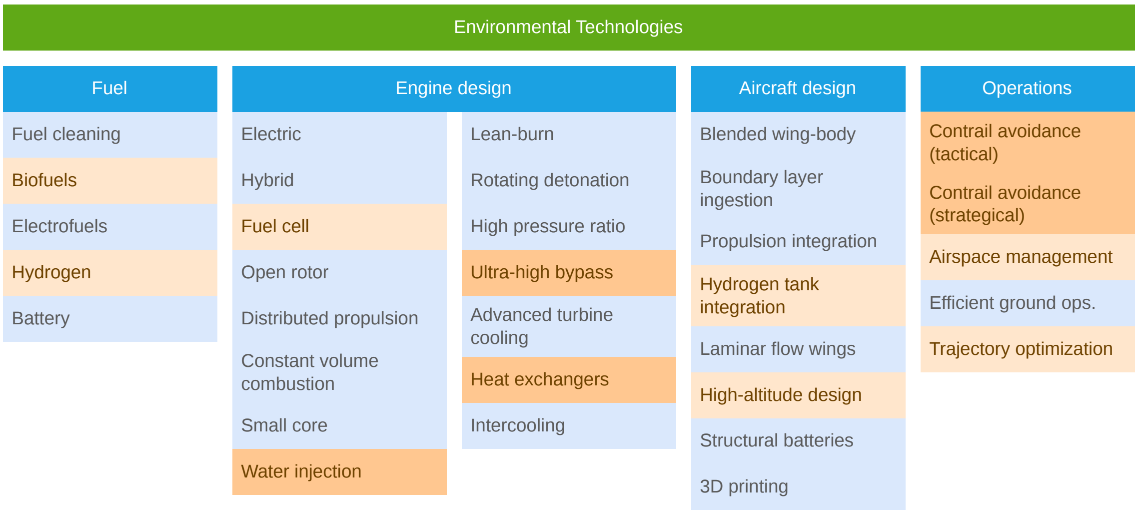

Figure 1.3: A selection of aviation technologies with a potential for reduced environmental impact. Dark orange represents technologies under investigation in this thesis. Light orange represent possible pathways for future investigations.

As with GWP, GTP and ATR can be expressed as CO_2 equivalents for easy comparison between different emissions.

Comparing short- and long-lived emission species is difficult and heavily dependent on the chosen time horizon. In an attempt to create a metric that can handle varying lifetimes while not requiring the selection of an arbitrary time horizon, the GWP* metric was developed. The original version only included methane, but the framework can be used for other short-lived species as well. However, GWP* has been criticized for being complicated to calculate and difficult to interpret.

1.4 Mitigation strategies

There are many technologies being investigated to minimize and mitigate the climate impact of aviation. In broad terms, they can be divided into five categories: fuel, propulsion architecture, engine design, aircraft design, operations. The categories and selected technologies within them are shown in Figure 1.3.

Substantial effort is devoted to research into new fuels. Biofuels are already available on the market today and are often made from used cooking oil, although other biological feedstocks can be used. Electrofuels are fuels with characteristics similar to Jet-A that are made from renewable feedstocks but require electricity to produce. Together these form what is known as sustainable aviation fuels (SAF). SAF is net zero in terms of CO_2 when considering the CO_2 captured from the atmosphere during fuel production and the CO_2 emitted during fuel combustion. However, production and transportation of SAF still results in CO_2 emissions. The non-CO_2 effects of SAF are similar to those of conventional jet fuel, although current research suggests that lower levels of soot are formed from SAF, which also has a positive effect on contrail mitigation [7]. A similar effect may be achieved using fuel cleaning, in which the sulfur and aromatic content of the fuel are reduced and the hydrogen-to-carbon ratio is increased [8].

Hydrogen has a higher energy density per mass than conventional jet fuel and can be produced from pure water using only electricity, making it an attractive choice to replace more conventional fuels. However, it has a low density, requiring large storage tanks. Integration of these tanks is a major aircraft design challenge, and some suggest novel designs such as the blended wing body in order to provide sufficient internal volume [9]. Hydrogen can either be combusted in a conventional aero-engine, if designed for that purpose, or could be used in a fuel cell to generate electricity. Combusting hydrogen instead of jet fuel eliminates CO_2 emissions and significantly reduces aerosol emissions, as formation of soot and sulfate particles is prevented [10]. Reduced particle numbers also has an effect on contrails, with an expected fleet-wide reduction in contrail EF of 70 % [11]. Using hydrogen in a fuel cell system, no NO_x is produced as the temperatures are too low. It may be possible to condense the water before it leaves the engine, resulting in larger droplets that quickly settle out of the stratosphere. A hybrid approach could be taken between combustion and fuel cell use of hydrogen to get a balance between power, weight and emissions.

As water and sulfate emissions are related to the fuel, engine designs mostly target reductions in CO_2, NO_x, and soot emissions. Lean-burn combustion is one concept that targets lower soot emissions. Previously, lower soot emissions were expected to result in decreased contrail forcing. However, a recent study has shown that lean-burn engines produce substantial contrail forcing, and that other technologies targeting vPM particles are needed as well [12]. Many concepts require a trade-off between different emissions. For example, high pressure ratio engines are more efficient and thus reduce fuel burn and CO_2 emissions, but the high pressure promotes NO_x formation. Other concepts trade reduced emissions for increased weight, and the challenge lies in finding a balance of plant such that the benefits are realized. One such concept is the Water Enhanced Turbofan (WET), in which water is injected into the combustion chamber and condensed after the turbines through large heat exchangers. The water injection lowers temperature in the combustion chamber, lowering NO_x formation, while at the same time increasing turbine work, allowing for ultra-high bypass and decreased fuel burn [13]. The recuperating heat exchangers also allows for water produced during combustion to be condensed, reducing SWV emissions and impeding contrail formation. The trade-off lies in the large and heavy heat exchangers, which increase drag and aircraft weight. More about this can be found in Chapter 3 and in Paper 1.

Operations primarily concern the efficiency of the air traffic and airport management. However, large operational climate benefits can be found through contrail avoidance and trajectory optimization. Tactical and pre-tactical contrail avoidance involve avoiding areas with weather patterns that are more likely to lead to contrail formation. This could be integrated into a trajectory optimization software, giving airlines direct authority over their climate impact. Strategic contrail avoidance involves planning air traffic in a way that, on average, lowers the likelihood of contrail formation. This could for example include scheduling more daytime flights rather than nighttime flights, or promoting travel during certain parts of the year. More about contrail avoidance can be found in Section 2.4.

1.5 Thesis purpose and outline

The purpose of the project is to investigate the climate impact of aviation and identify effective strategies to mitigate it, with particular emphasis on non-CO_2 emissions and contrail formation. This work aims to evaluate the relative importance of different contributing factors and to explore the potential of technological and operational measures in reducing aviation's climate footprint. By assessing the feasibility and environmental benefits of promising solutions, this work seeks to support the development of more sustainable aviation practices and inform future research in this field.

The thesis is structured as follows. Chapter 2 addresses contrails, the dominant non-CO_2 effect of aviation. It introduces the mechanisms of contrail formation and their climate impact, followed by an overview of available modeling approaches and their associated uncertainties. The chapter concludes with a discussion of mitigation strategies, serving as a foundation for future research in this area. Chapter 3 investigates the Water Enhanced Turbofan (WET) concept as a potential pathway toward more climate-friendly aviation. The chapter begins by outlining the fundamental principles of the cycle, followed by a discussion of its key constraints and limitations. The potential environmental benefits of the concept are then assessed. Finally, the chapter presents the modeling framework used to analyze the WET engine, encompassing all relevant components and system-level considerations. The appended papers further support the work presented in this thesis. Paper 1 examines the thermodynamic feasibility of the WET engine, while Paper 2 analyzes the climate impact of Swedish aviation, with particular emphasis on contrail effects.

Chapter 2

Contrails

2.1 Formation

In simple terms, contrails are man-made clouds of ice particles, and they form when a pocket of air contains more water than it can normally hold, a condition known as supersaturation. Another requirement is nucleation sites, which are particles that the water can attach to. If there are no available nucleation sites, the atmosphere can become supersaturated.

There are two types of supersaturation, depending on the type of nucleation sites. In ice-supersaturation, water in the air would start to deposit if an ice surface were available. In liquid-supersaturation, water would start to condense if a liquid surface were available. Notably, in liquid supersaturation, water can condense on a wide range of particles, whereas in ice supersaturation, ice formation typically requires specific ice-nucleating particles or sufficiently low temperatures. In Figure 2.1, the saturation lines for ice and liquid water are illustrated over a range of ambient

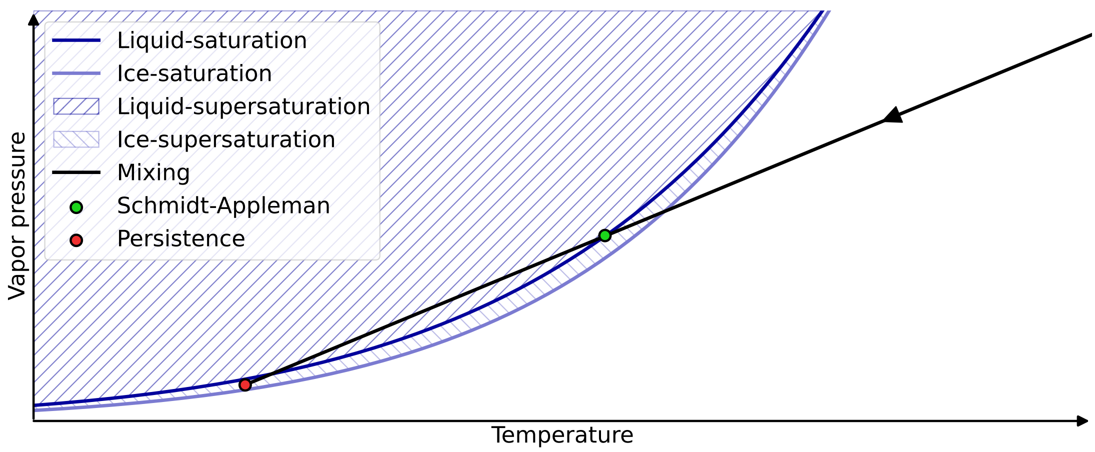

Figure 2.1: Illustration of the necessary requirements for persistent contrails. The mixing line between the exhaust and the ambient air crosses the liquid-saturation line, termed the Schmidt-Appleman criterion, causing a contrail to form. The line terminates in an ice-supersaturated state, causing the contrail to persist.

temperatures. The warmer the air is, the more water it can hold before it becomes saturated. Also note that the liquid-saturation line is at a higher water concentration than the ice-saturation line.

Air exiting an aircraft engine is hot and humid due to the combustion process. As it mixes with the surrounding air, the temperature and water concentration drop until it is fully mixed, at which point ambient conditions are reached. The mixing process is exemplified in Figure 2.1 by the mixing line, which is a straight line from the engine conditions to the ambient conditions. For contrails to form, the mixing line needs to cross the liquid-saturation line [14, 15]. This is called the Schmidt-Appleman criterion. At the point when liquid-saturation is reached, liquid water droplets begin to form with aerosols acting as nucleation sites. These aerosols can be the nvPM and vPM particles discussed in Section 1.2.4, but can also be ambient aerosols present in the atmosphere. When the liquid droplets form, they immediately freeze due to the cold atmospheric temperatures. Once the ice particles have formed, they grow as more ice is deposited on them.

The vast majority of the forcing from contrails comes from persistent contrails. These contrails stay in the atmosphere for long periods of time, sometimes several hours, whereas non-persistent contrails sublimate shortly after they are formed. Whether a contrail is persistent or not depends on the ambient conditions. If the local ambient conditions are ice-supersaturated, the contrail will persist. Otherwise, mixing will eventually lower the local humidity below the ice-supersaturation threshold, causing the ice particles to sublimate. A part of the atmosphere that is ice-supersaturated is called an ice-supersaturated region (ISSR).

To summarize, persistent contrail formation requires two conditions. The first is that the local properties in the engine exhaust at some point cross the liquid-saturation line during mixing. The second is that the contrail is formed within an ISSR. The exact ambient temperature, humidity, and wind, as well as the temperature, humidity, and number of particles in the exhaust, determine detailed contrail properties such as how long they persist, how wide they become and how much forcing they contribute.

2.2 Climate impact

Each contrail is unique and its properties determine the climate impact. Among the important properties are

- how long and wide it becomes,
- the persistence/lifetime of the contrail,
- how it interacts with short-wave (solar) and long-wave (heat) radiation,
- the time of day,
- whether other contrails or clouds cover the same area,
- and whether contrail-induced cirrus clouds form or not.

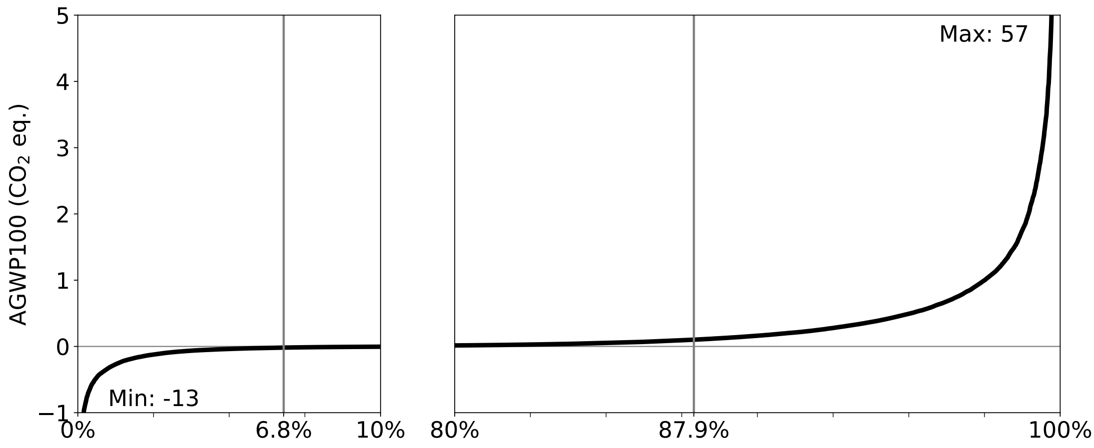

Figure 2.2: Distribution of contrail climate impact for flights departing from and arriving at Arlanda airport in 2025. 6.8 % of the flights are responsible for 95 % of the cooling effect, while 12.1 % are responsible for 95 % of the warming effect. The maximum cooling was -13 CO_2 eq. and the maximum warming was 57 CO_2 eq.

These factors can broadly be described in terms of contrail area, lifetime, and opacity, as well as the background radiation, other cloud layers affecting radiation, and whether large clouds are formed. Contrail-induced cirrus clouds are estimated to be responsible for 90 % of the radiative forcing from contrails [6] and are thus a very important effect.

The climate impact is not distributed evenly between flights. Figure 2.2 displays the distribution in contrail energy forcing (EF) per flight, as compared to the CO_2 energy forcing. The data is taken for flights departing from and arriving at Arlanda airport during 2025, and is presented in Paper 2. Only 12 % of flights cause 95 % of the warming effect. Most flights do not have a significant contrail energy forcing, with more than half not forming a contrail at all. Although the probability of forming a highly warming contrail is small, the effect can be huge when it is formed. One of the analyzed flights had a contrail climate impact that was more than 50 times larger than the impact from the CO_2 emitted. Such flights are often termed "big hits" and are especially important for mitigation, as a very large climate impact can be avoided with minimal additional fuel burn and minor delays. This is discussed further in Section 2.4. It should also be noted that some flights produce significant cooling forcing. Increasing the occurrence of cooling contrails is one way to reduce the net anthropogenic warming impact. However, oftentimes such proposals are regarded as ill-advised due to the large uncertainty in contrail forcing.

Climate impact can not be represented by a single number. Rather, it is a concept than can be measured in multiple ways, as illustrated by the large number of climate metrics (nine, excluding time horizons) discussed in Section 1.3. Contrails are a short-lived effect, meaning that they have a large radiative forcing for a short period of time. This is in contrast to, for example, CO_2, which has an atmospheric lifetime exceeding 100 years. The metric and time horizon chosen therefore introduce a bias in how short-term and long-term effects are weighted. For climate change, temperature is generally considered to matter more than raw forcing. However, the temperature response is not linearly related to the forcing. Generally, scenarios are required to properly evaluate the temperature response. To complicate matters further, one can consider the temperature at a given time, the equilibrium temperature, or the maximum temperature reached.

Even when a certain metric can be decided upon, the uncertainties involved are large. Lee et al. estimate that the global ERF contribution from contrails is 167 % of the CO_2 ERF [6]. When uncertainties are included, taking the lower bound of the contrail ERF and the upper bound of the CO_2 ERF, the value shrinks to 43 %. On the other hand, the uncertainty is large in both directions, and it is equally plausible that the contrail ERF is 350 % of the CO_2 ERF.

2.3 Prediction and modeling

Calculating the contrail forcing produced by past flights and predicting the forcing from future flights require models and measured data, the quality and accuracy of which are of great importance. Section 2.3.1 describes CoCiP, the current state-of-the-art model used for contrail prediction. Sections 2.3.2, 2.3.3 and 2.3.4 describe the input data needed to run CoCiP in addition to trajectory data.

2.3.1 CoCiP

The Contrail Cirrus Prediction model (CoCiP) was originally developed by U. Schumann [16]. The CoCiP model assumes that particles from the engine exhaust spread out according to a Gaussian distribution. Given that contrail-forming conditions are met, the initial ice crystal mass and number of particles are calculated, and these are advected using a time-stepping procedure. Finally, the effect of the ice particles on long-wave and short-wave radiation is calculated. Since its initial publication, the model has been updated and incorporated into the Python library pycontrails [17–21], together with complementary tools for processing flight data.

A typical workflow surrounding CoCiP can be seen in Figure 2.3. CoCiP operates on trajectory data, where each point along the trajectory includes the latitude, longitude, altitude, and true airspeed of the aircraft. The trajectory data may be obtained from open sources such as the OpenSky Network [22], which collects ADS-B messages sent by aircraft around the world through receivers operated by volunteers. Additionally, CoCiP requires the fuel flow to be known at each point. For most research purposes, such data is not available. Therefore, an aircraft performance model is necessary. CoCiP also requires the emission index for nvPM, which is generally estimated due to the difficulty of performing in-flight measurements. CoCiP then intersects the trajectory with weather data. After that, all parameters are extracted and CoCiP can run its internal calculations.

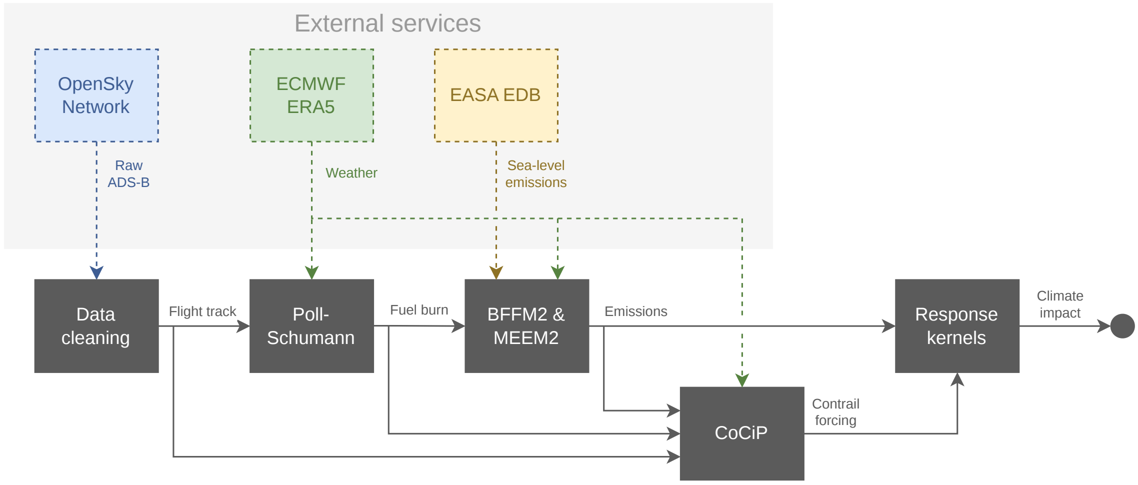

Figure 2.3: Flowchart depicting how CoCiP is typically used in conjunction with other models and data sources to calculate contrail forcing. In this particular case, other emissions are also estimated using the Boeing Fuel Flow Method (BFFM2) and their climate impact is calculated using response kernels.

2.3.2 Aircraft performance

Aircraft performance models take trajectory data and estimates performance parameters such as overall engine efficiency and fuel flow. There are multiple aircraft performance models to choose from, with varying levels of detail, accuracy, and computational cost.

For large studies, a common aircraft performance model is the Base of Aircraft Data (BADA) model developed by EUROCONTROL [23]. It uses empirical equations, assuming that performance varies linearly with altitude and speed, and divides the flight into climb, cruise, and descent, with special treatment of landing and take-off (LTO). It requires proprietary constants for each aircraft and engine configuration, and these are licensed from EUROCONTROL.

Another option, which is openly available and does not require proprietary constants, is the Poll-Schumann model [24, 25]. It uses simplified equations derived from thermodynamic principles. It still requires constants for each aircraft and engine configuration, but these constants are provided. It has been shown to have slightly improved performance compared to BADA3, with a mean absolute percentage error of 8.6 % [26].

2.3.3 Particle emissions

Broadly, contrail forcing scales linearly with the number of ice nucleation sites. Accurate calculation of the number of particles in the exhaust is therfore essential for understanding the climate impact of contrails. Unfortunately, particle emissions are difficult to measure in flight, and one must instead rely on certification data obtained through sea level static tests. These LTO certification tests are conducted for all jet and turbofan engines used in aviation with thrust above 26.7 kN. The simplest approach is to assume a constant emission level throughout all phases of

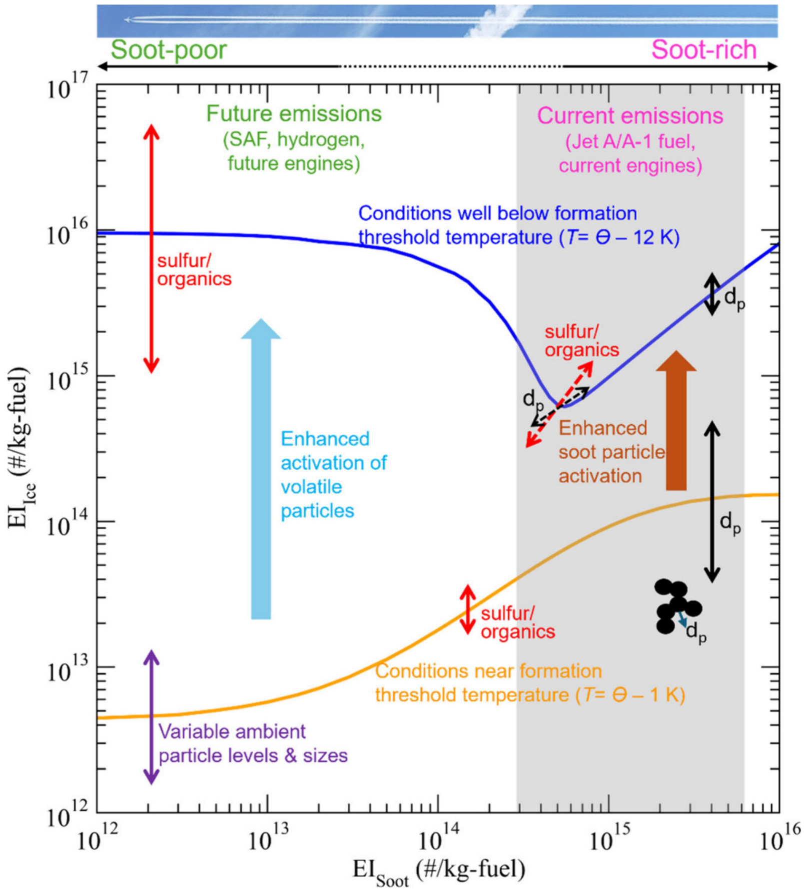

Figure 2.4: Visualization of the ice particle formation process, including the effect of volatile particulate matter (vPM). In cold conditions, low-soot engines can produce more ice particles due to the increased activation of vPM. Created by Yu et al. [27].

flight based on the certification data. A more advanced method, called the nvPM Mission Emissions Estimation Methodology (MEEM2) [28, 29], interpolates on thrust in the LTO certification data and scales the result using the ambient temperature and pressure. To date, no literature exists comparing this model to experimental data in critical phases of flight. However, comparisons with original equipment manufacturer (OEM) proprietary models show that MEEM2 can both overpredict and underpredict depending on the engine and the mission phase. It should also be noted that this model only concerns nvPM particles. vPM has recently been shown to have a large effect on ice particle formation, as is visualized in Figure 2.4. In low-soot scenarios, the effect of vPM particles can even outweigh that of nvPM particles [27].

2.3.4 Weather forecast and reanalysis

Weather is notoriously difficult to predict. There are fundamental limits to how well something can be predicted in a chaotic system, such as the atmosphere, and today's weather forecasting models are closing in on that limit. However, knowing the past weather is not trivial either. Aircraft fly at high altitudes where no permanent

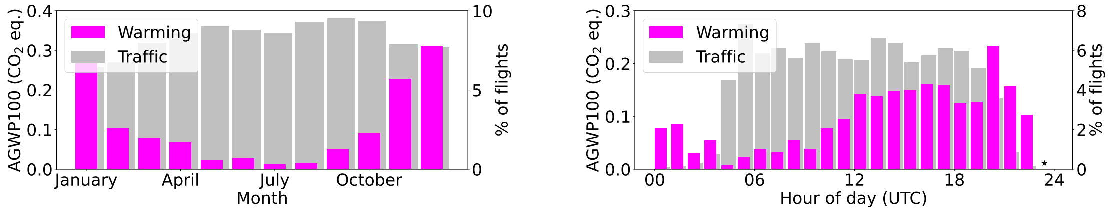

(a) Monthly (b) Hourly

Figure 2.5: Contrail warming and number of flights for flights departing from or arriving at Arlanda airport in 2025, displayed by departure time. The time slot marked with a ⋆-symbol was omitted due to there being fewer than 100 flights in total.

weather stations exist. Instead, datasets on past weather, called reanalysis data, rely on measurements taken by ground stations and weather balloons, combined with advanced thermofluid dynamical models.

The most important thing to predict for contrail research is the presence of ISSRs. How accurate a weather model is in predicting the presence of ISSRs can be measured by hit rate and false alarm rate. The hit rate measures how many known ISSRs the weather model accurately predicts. The false alarm rate measures how many predicted ISSRs were not observed by measurements. Rädel et al. studied the accuracy of ECMWF IFS forecasts and found that, for a 1-day forecast with 3 km vertical resolution, the hit-rate of ISSRs was 76 % and the false alarm rate was 15 % [30]. For a 3-day forecast, the hit rate decreased to 68 % and the false alarm rate increased to 20 %. Improving the vertical resolution in the data to 0.3 km reduced the false alarm-rate but also reduced the hit rate significantly.

2.4 Avoidance

Contrail avoidance refers to attempts to prevent contrail formation by adjusting how, when, and where one or more aircraft fly. It is divided into three categories: strategic, pre-tactical, and tactical.

Strategic contrail avoidance occurs at a very early stage, long before the aircraft departs. It involves analyzing weather data and past contrail-forming flights to identify trends that can be leveraged. The results of such analyses may be used to establish general recommendations. One example is shown in Figure 2.5, which displays the number of flights and their resulting contrail forcing, partitioned by month (left) and hour of departure (right). The analyzed flights include all the commercial jet airliner flights departing from or arriving at Arlanda airport in Stockholm during 2025. It is clear that, although traffic is fairly evenly distributed throughout the year, the contrail forcing is significantly more pronounced in winter than in summer. In fact, the contrail forcing from the month with the highest forcing is 25 times larger than the forcing from the month with the lowest forcing. The hourly breakdown shows that early morning flights have very little climate impact from contrails, whereas evening and night flights have a much more pronounced

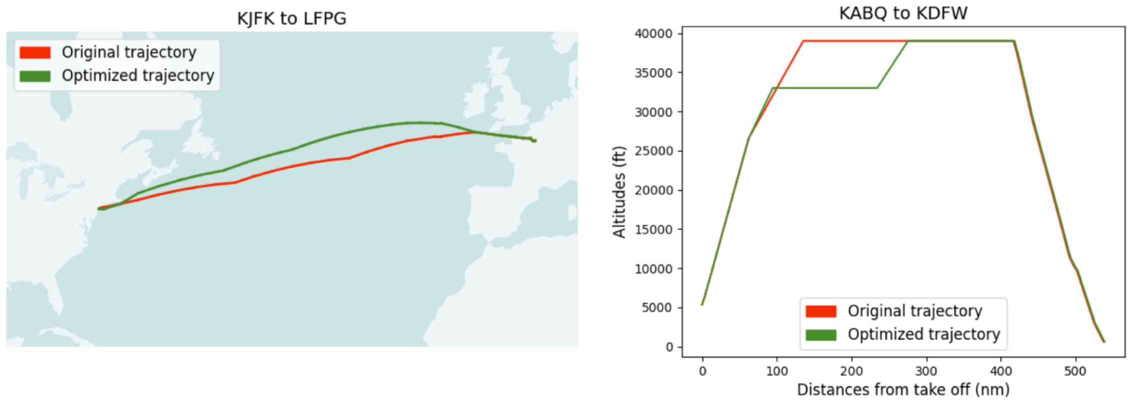

(a) Horizontal deviation (b) Vertical deviation

Figure 2.6: Flight trajectories before and after optimizing for minimum contrail forcing, using horizontal diversions (left) and vertical diversions (right). Created by Frias et al. [31].

effect. These insights can be used to promote flights in summer over winter flights, or to encourage early morning departures instead of night flights.

Pre-tactical contrail avoidance occurs from a couple of days before departure up to a few hours before the flight, when the flight plan is created and updated. At this stage, weather forecasts can be utilized to prevent flying over areas with a high risk for contrail formation, either through re-routing the aircraft laterally, adjusting the flight altitude or by changing the time of departure. An example of a lateral diversion and an altitude diversion is illustrated in Figure 2.6. Typically, adjusting the flight altitude is the most common approach, as it has been shown to result in lower additional fuel burn than lateral adjustments and avoids delays [32]. The flight plan is continually updated as improved weather forecast and data regarding booking density and airport load become available. Pre-tactical contrail avoidance has a low operational load on air traffic controllers, as it gives them time to plan accordingly. However, it relies on predictions and is therefore susceptible to model and weather uncertainties.

Tactical contrail avoidance occurs during the flight. It is typically initiated by the pilot but could also be initiated by air traffic controllers. Tactical avoidance is primarily applied when a visual contrail is formed behind the aircraft, and this can happen even when pre-tactical avoidance is applied due to prediction uncertainties. The pilot may then request an altitude adjustment to find a region of the atmosphere that does not form contrails. This method relies only on observable data, ensuring that only flights that form contrails are affected. However, it affects all contrail-forming flights equally, regardless of the potential climate impact they may have. To reduce operational costs, avoidance should ideally be applied only to flights with substantial forcing. Moreover, changing the route during flight increases the workload on air traffic controllers, especially when multiple aircraft need to avoid the same area.

Chapter 3

Water Enhanced Turbofan

The Water Enhanced Turbofan (WET) is a proposed future engine cycle that was first described by Schmitz et al. in a series of papers on future engine technologies [13, 33, 34]. It is a combination of the Joule-Brayton cycle of a typical turbofan and the Cheng cycle [35]. It utilizes water injection for improved cycle efficiency, reduced NO_x emissions, and reduced contrail formation. The water is then recuperated through two heat exchangers, called the vaporizer and the condenser. If the benefits of the WET engine are realized, it could be an important step towards climate-friendly aviation.

3.1 Engine architecture

3.1.1 Turbofan

The WET engine is a turbofan engine that has been augmented with a water/steam loop. In a turbofan engine, air enters the engine through the fan, which pressurizes it and accelerates it downstream. The air is then divided into a core stream and a bypass stream, and the ratio of the mass flow of air going into either stream is called the bypass ratio (BPR). In the smaller core stream, the air is heavily compressed in multiple stages and then combusted together with fuel, after which power is extracted through turbines. The power from the turbines is used to drive the compressors and the fan. Thrust is generated from both the core and the bypass stream as air exits through their respective nozzles. On modern engines, there are two to three compressors (including the fan) and two to three turbines present. The compressors and turbines can all be connected by a single shaft. In that case, a gearbox is required so that the fan can rotate at a lower speed than the rest of the turbomachinery components. The compressors and turbines can also be connected on different shafts that rotate freely, which allows for the rotational speeds to be set independently.

The efficiency of a turbofan can be divided into two parts, the propulsive efficiency (η_{pr}) and the thermal efficiency (η_{th}). Together, they form the overall efficiency of the cycle:

$$\eta_{\mathrm{o}} = \eta_{\mathrm{pr}}\, \eta_{\mathrm{th}}. \tag{3.1}$$

The propulsive efficiency describes how well kinetic energy in the flow is turned into thrust. It is defined as

$$\eta_{\mathrm{pr}} = \frac{F\, c_0}{\dot{W}_{\mathrm{kin}}}, \tag{3.2}$$

where F is the thrust generated, c_0 is the aircraft velocity, and $\dot{W}_{\mathrm{kin}}$ is the kinetic energy flow rate. For a single jet, it can be approximated as

$$\eta_{\mathrm{pr}} = \frac{2}{1 + \frac{c_9}{c_0}}, \tag{3.3}$$

where c_9 is the velocity of the flow as it comes out through the nozzle. Since the flow has a lower velocity as it exits the bypass nozzle than the core nozzle, the bypass stream has a higher propulsive efficiency than the core stream. Thus, for high propulsive efficiency, a high BPR is desirable. However, BPR is limited by the power that the core can supply. This is discussed further in Section 3.2.

Thermal efficiency on the other hand describes how well chemical energy is turned into kinetic energy. It is defined as

$$\eta_{\mathrm{th}} = \frac{\dot{W}_{\mathrm{kin}}}{\dot{m}_{\mathrm{f}}\, \mathrm{LHV}}, \tag{3.4}$$

where $\dot{m}_{\mathrm{f}}$ is the fuel flow rate and LHV is the lower heating value of the fuel. The thermal efficiency depends on the internal losses throughout the engine and is thus highly dependent on the efficiency of the individual turbomachinery components.

A more tangible performance metric for a turbofan engine is the thrust specific fuel consumption (TSFC), defined as

$$\mathrm{TSFC} = \frac{\dot{m}_{\mathrm{f}}}{F}. \tag{3.5}$$

It expresses how large fuel flow is required to generate a certain thrust. A lower value means that less fuel is used to produce the same amount of thrust, indicating a more efficient engine. However, it doesn't include the weight of the engine and the drag it induces. For that, an aircraft with the engine installed needs to be analyzed. A simple metric that can be used in that case is the specific range (SR), defined as

$$\mathrm{SR} = \frac{c_0}{\dot{m}_{\mathrm{f}}}. \tag{3.6}$$

It expresses how far the aircraft gets per mass of fuel that is used. A larger engine will increase the weight and drag of the aircraft, requiring more thrust and thus increasing the fuel flow. More fuel flow for the same speed gives a lower SR.

3.1.2 Water injection and recuperation

A diagram of the WET engine can be seen in Figure 3.1. The core stream exits the turbines and enters the vaporizer at station 5. Cooled core air exits the vaporizer and enters the condenser at station 6. Core air with condensed water exits the condenser

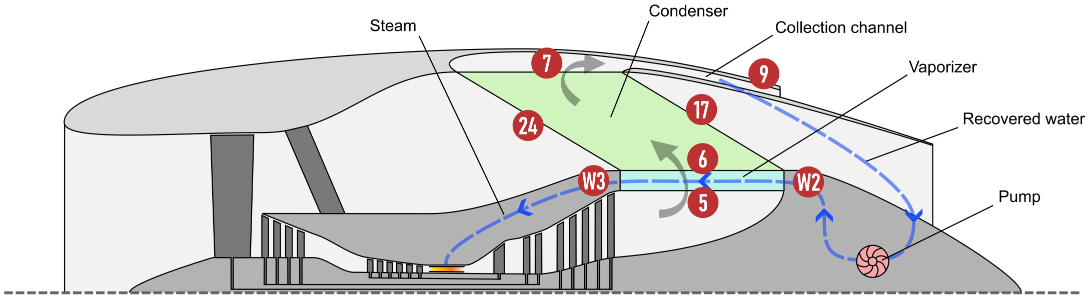

Figure 3.1: Diagram of the Water Enhanced Turbofan (WET) engine with key station numbers and components marked [36].

and enters the collection channel at station 7, and exits the engine through the core nozzle at station 9. The liquid water is collected in station 9 and is pumped to station W2 where it enters the vaporizer. At station W3, superheated steam exits the vaporizer, after which it is injected into the combustion chamber. Bypass air crosses the condenser from station 24 to station 17, cooling the core flow.

The main benefits of the WET engine lie in water injection. The amount of power that the core can generate is limited by the combustion temperature. By injecting steam into the combustion chamber, the core stream is cooled down. A cooler combustion process results in less NO_x production. However, the lower temperature also allows more fuel to be injected, thereby raising the temperature and increasing the power output. At the same time, the specific heat capacity of steam is higher than that of air, which amplifies this effect. The increased power in the core allows for a larger fan and thus a higher BPR, which improves the propulsive efficiency. In addition, the increased specific heat capacity reduces the losses in the turbines, improving the thermal efficiency. There is a trade-off between improvement in cycle efficiency and reduced NO_x emissions.

The cycle relies on a continuous injection of steam, and to avoid excessively large water tanks, the injected water must be recuperated for reuse. Therefore, two heat exchangers are installed on the engine. These can be seen in Figure 3.1 as a blue rectangle and a green parallelogram. The first heat exchanger encountered by the core flow is the vaporizer (blue), which is located immediately downstream of the turbines. The vaporizer cools the humid core flow by transferring heat to liquid water. This has the added benefit of preconditioning the water before it is injected into the combustion chamber by vaporizing it and superheating the steam. The cooled core air then encounters the second heat exchanger, called the condenser. In the condenser, the humid core air is cooled further until the water condenses out and is collected in a collection channel as liquid water. The coolant is the bypass air, which is close in temperature to the ambient air. When the ambient temperature is high, such as at sea level, the condenser cannot recover sufficient water, and water must instead be supplied from a tank.

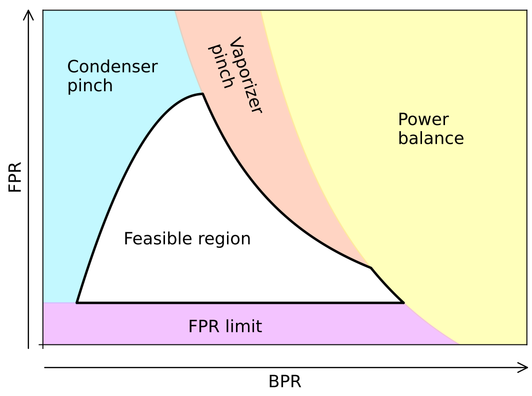

Figure 3.2: Diagram in the bypass ratio (BPR) and fan pressure ratio (FPR) domain, displaying the most important constraints affecting the WET cycle [36]. The constraints are set by heat exchanger performance, system power balance and fan efficiency.

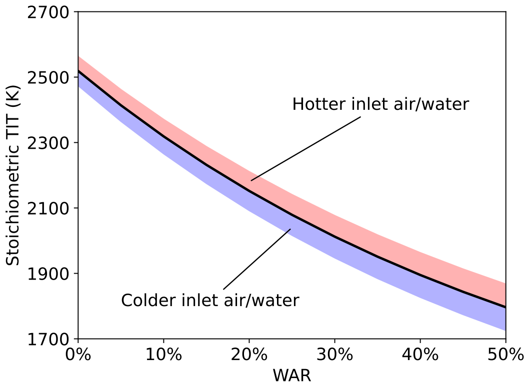

Figure 3.3: Maximum achievable turbine inlet temperature (TIT) as a function of the water-air ratio (WAR) [36]. High WAR leads to high dilution of the air in the combustion chamber, which lowers the temperature. The blue and red regions represent cold (<600 K) and hot (>600 K) inlet air and water, respectively.

3.2 Thermodynamic constraints

The WET cycle is constrained by multiple factors, some of which are novel and not present in typical turbofan engines. An illustration of how a selection of constraints impacts BPR and fan pressure ratio (FPR) can be seen in Figure 3.2. The primary constraint that affects both the WET engine and conventional turbofans is power balance. It states that all the power required by the fan and the compressors must be extracted from the core flow by the turbines. The core has a limited amount of extractable power, equal to the energy in the injected fuel minus losses in the turbines. Increasing BPR results in a larger fan for a fixed core, which requires more power. Similarly, a higher FPR increases the work performed by the fan, which also requires more power. Another constraint present in conventional turbofans is a lower limit on the design FPR. Very low FPR leads to excessive losses in the fan, and high fan efficiency is important as it is the component generating most of the thrust. Thus, there is a practical lower limit to FPR for achieving reasonable efficiency.

For the WET cycle specifically, the added heat exchangers impose new limitations. The heat exchangers increase the engine weight and add pressure losses to both the core and the bypass stream, which reduces overall efficiency. There is a trade-off between size, weight, and pressure losses, which requires careful attention when designing the heat exchangers. However, a strict constraint is imposed due to the heat exchanger pinch temperature. In each heat exchanger, there is a cold channel and a hot channel, and heat is transferred from the hot channel to the cold channel. The lowest temperature difference between these channels along the length of the heat exchanger is called the pinch temperature. For the heat exchanger to be physically meaningful, the pinch temperature must be positive. Otherwise heat would naturally flow in the opposite direction. Thus, the possible combinations of inlet and outlet temperatures are limited. However, as the vaporizer and condenser handle very different processes, the corresponding pinch constraints differ significantly in the BPR-FPR domain.

Additionally, the temperature of the combustion chamber exhaust, also known as the turbine inlet temperature (TIT), cannot be set arbitrarily. The highest temperature is achieved when a stoichiometric mixture of fuel and air is combusted, as all the oxygen is used. Any higher fuel-air ratio (FAR) will lead to incomplete combustion and a lower combustion temperature. This disregards uneven combustion, which further decreases the maximum TIT. The injection of steam into the combustion chamber introduces an additional dimension to this constraint, as the steam cools the combustion process, as shown in Figure 3.3. At high water-air ratios (WAR) of 50 %, the maximum TIT dips below 1900 K. However, for a fixed amount of air and fuel, the addition of steam does not affect the power available for extraction, despite lowering the temperature of the gas mixture.

Finally, due to the higher specific heat capacity of water compared to air, the temperature decreases more slowly as the flow passes through the turbines. High temperatures can thus reach further down into the turbine system, requiring cooling of turbine stages which were previously not cooled. This adds complexity and weight, limits the amount fuel which can be injected, and decreases the efficiency of the turbines.

3.3 Performance and environmental benefits

The original article by Schmitz et al. suggested that the total fuel burn reduction potential for the WET engine is about 15 % [13]. Schmitz et al. also discussed non-CO_2 emissions and suggested that complete avoidance of NO_x emissions could be achieved, together with a significant reduction in contrails and a modest reduction in soot. The presence of water and the lower temperatures in the combustion chamber were thought to completely eliminate NO_x emissions, as NO_x formation requires high temperatures and access to N_2 and O_2. The condensation and collection of water, together with the comparatively small core, were cited as the reasons for the reduction in contrails, as less water would be emitted. Soot particle emissions would also be reduced, as some particles would follow the water during condensation.

A later study by Kaiser et al. further examined the emissions reduction potential using a more advanced thermodynamic turbofan model, coupled with models for estimating the reductions in NO_x and contrails [37]. Their results are summarized in Figure 3.4. They estimated that TSFC could be reduced by 13 %, resulting in a fuel burn reduction of 10 % after accounting for installation effects. NO_x emissions were estimated to be reduced by more than 90 %, and contrail forcing by over 50 %. In total, the climate impact would be reduced by more than 40 %.

Paper 1 evaluates the cycle independently of Schmitz et al. and Kaiser et al., focusing on performance and fuel consumption. The thermodynamic model employed includes a state-of-the-art, early design tool for heat exchangers, giving an estimation of the pressure loss, size and weight of the heat exchangers. It also includes treatment

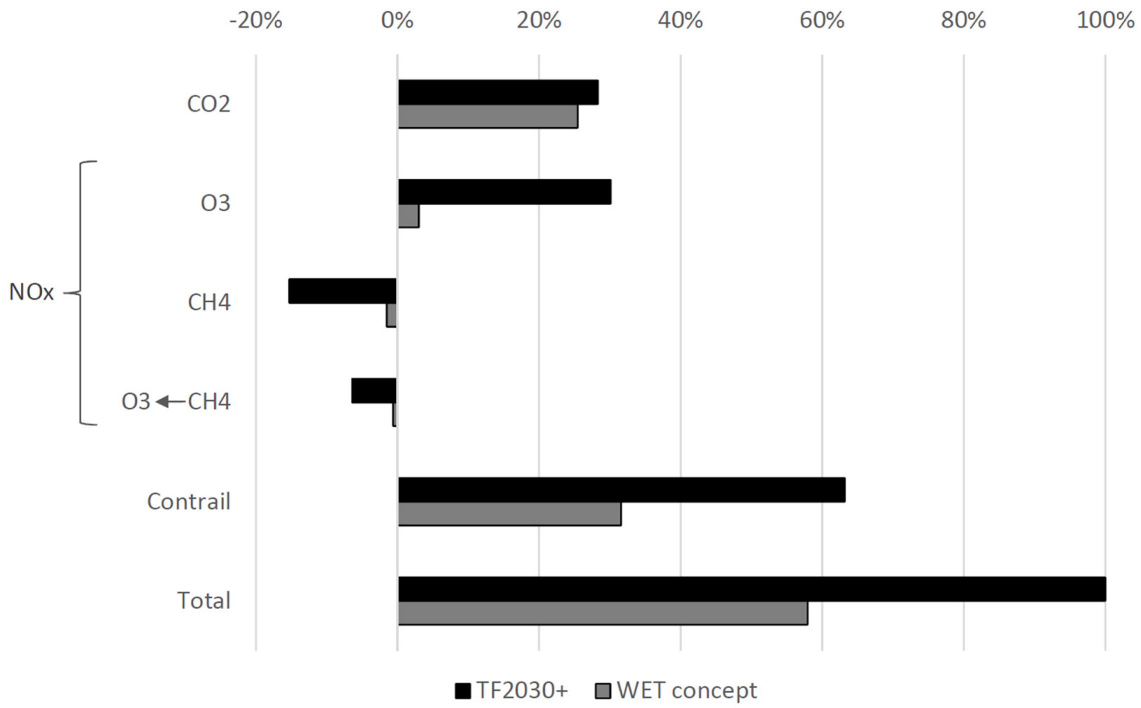

Figure 3.4: Climate impact assessment for the WET engine compared to a conventional turbofan with entry into service in 2030, produced by Kaiser et al. [37]. The scale is in AGWP100 and is normalized towards the total AGWP100 of the conventional turbofan.

of installation effects derived from aircraft conceptual design methodologies and first-order principles. More on the modeling can be found in Section 3.4. The main results presented in Paper 1 are:

- Cooling of the low pressure turbine may be required for multiple stages due to the increased specific heat capacity of the core, increasing complexity and weight of the core.
- For best performance, the cycle needs to be designed for high water injection of 30 %, requiring large water storage tanks or very high turbine inlet temperatures for take-off.
- Even with optimal cycle parameters, the engine burns more fuel compared to a modern reference engine.

The performance of the optimized WET engine from Paper 1 are summarized in Figure 3.5. It shows that, for an engine optimized for fuel burn, the cycle efficiency is significantly improved. In total, TSFC increases by 18 % compared to the reference engine [36]. However, when accounting for pressure losses in the heat exchangers, the drag from the larger nacelle, as well as the weight of the heat exchangers, nacelle, and water tank, the WET engine achieves a SR that is 8.8 % lower than the reference. For this optimized engine, the combustion temperature in cruise is higher than that of the reference, negating some of the impact of water injection on reducing NO_x

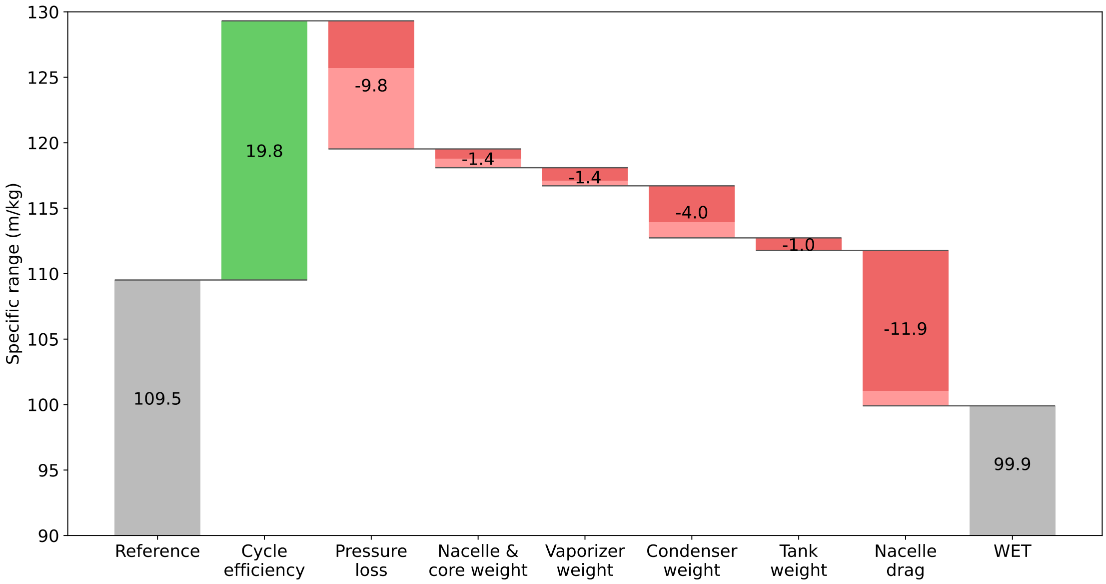

Figure 3.5: Waterfall chart displaying the specific range (SR) of the WET engine compared to a reference engine and the aspects that cause the difference.

formation. The optimized engine also has a condenser sized to provide exactly the required amount of water in cruise. No excess water is condensed, so the impact of the cycle on contrails is limited to potential reductions in particle emissions. Thus, all emissions are revised upward significantly compared to the estimates by Kaiser et al.

3.4 Modeling

3.4.1 Turbomachinery

Turbofan engines typically contain multiple sets of compressors and turbines, which are turbomachinery components. The fan is also a compressor, albeit with a much lower pressure ratio and rotational speed than the other compressors. Compressors and turbines can be modeled using the polytropic equations [38], stating that

$$\frac{T_{02}}{T_{01}} = \left(\frac{p_{02}}{p_{01}}\right)^{\frac{\gamma-1}{\gamma\,\eta_\mathrm{p}}}, \tag{3.7}$$

for compressors, and

$$\frac{T_{02}}{T_{01}} = \left(\frac{p_{02}}{p_{01}}\right)^{\frac{(\gamma-1)\,\eta_\mathrm{p}}{\gamma}}, \tag{3.8}$$

for turbines. In the above equations, T_{01} and T_{02} are the total temperature before and after the component, p_{01} and p_{02} are the total pressure before and after the component, γ is the ratio of specific heats, and η_p is the polytropic efficiency. For a given turbomachine, the polytropic efficiency at a certain operating point can be determined from a compressor map or turbine map. These map efficiency as a function of corrected speed ($\frac{\Omega}{T_{01}}$) and corrected flow ($\frac{\dot{m}\sqrt{T_{01}}}{p_{01}}$). Here, Ω is the rotational speed of the component and $\dot{m}$ is the mass flow of gas through the component. Compressor maps also determine the pressure increase ($\frac{p_{02}}{p_{01}}$) over the compressor. The rotational speed of turbomachines connected on the same shaft must always match, except for when a gearbox is introduced. Geared turbofan engines often have a gearbox with a fixed gear ratio.

The simplest way to model ducts, inlets, and nozzles is to use the isentropic relation, assuming no losses:

$$\frac{T_{02}}{T_{01}} = \left(\frac{p_{02}}{p_{01}}\right)^{\frac{\gamma-1}{\gamma}}. \tag{3.9}$$

However, losses can also be included through a fixed pressure drop, a pressure recovery factor, or an isentropic nozzle efficiency.

A turbofan engine also includes other subsystems which require modeling for accurate results. Some of the turbine stages need cooling, which is done by taking air from the high pressure compressor. Air is also taken from the compressors to drive the hydraulic system and for use in the air conditioning system. Furthermore, electrical power is generated from one of the shafts, reducing the available power for the compressors. More detailed discussion on the modeling of turbomachinery components can be found in the thesis by Grönstedt [39].

3.4.2 Heat exchanger

On a conceptual level, a heat exchanger consists of two channels containing fluids with a solid interface in between. Heat is transferred from the hot fluid to the cold fluid via conduction through the solid wall. The process of heat transfer can be described by the logarithmic mean temperature difference (LMTD) method, which states that the heat transfer $\dot{Q}$ can be expressed as

$$\dot{Q} = U \cdot A \cdot \text{LMTD}, \tag{3.10}$$

where U is the heat transfer coefficient and A is the surface area of the internal channel in which the heat transfer takes place. The LMTD is expressed as

$$\text{LMTD} = \frac{\Delta T_{\text{A}} - \Delta T_{\text{B}}}{\ln(\Delta T_{\text{A}}) - \ln(\Delta T_{\text{B}})}, \tag{3.11}$$

where ΔT_{A} and ΔT_{B} are the temperature differences between the two channels at either end of the heat exchanger.

To determine the heat transfer coefficient, one has traditionally had to use specific equations for each type of heat exchanger, often requiring detailed knowledge of the design. However, recent advances in compact heat exchanger modeling have made it significantly easier to model the performance of state-of-the-art heat exchangers. In particular, the GenHEX method developed by Miltén et al. [40] has made it possible to estimate the heat transfer coefficient of heat exchangers, as well as the pressure drop and weight, at an early concept level. It utilizes three non-dimensional, generalized geometric parameters (GGP) as design inputs. These are the surface-area-density ratio (α_r), the void-fraction ratio (σ_r) and the compactness fraction (χ). It is also necessary to know the external dimensions of the heat exchanger, the mass flow rate of fluid in each of the channels, and some additional geometric parameters.

The GGPs directly give the weight of the bulk material for the heat exchangers through geometric relationships. For the heat transfer coefficient and pressure drop, GenHEX employs empirical correlations derived from tests on compact heat exchangers. Using these equations, the GGPs can be varied freely to find an optimal trade-off between weight, heat transfer and pressure drop.

3.4.3 Installation effects

The most efficient engine is not necessarily the engine that burns the least amount of fuel for a given mission. An engine with higher drag requires more thrust to counteract it, which increases fuel burn. A heavier engine increases the lift requirement of the aircraft, which necessitates larger wings, thereby increasing drag and, by extension, fuel burn. These effects, termed installation effects, are important to consider when large modifications are investigated, such as for the WET engine.

Aircraft weight (w_{AC}) can be divided into wing (w_{wing}), fuselage (w_{fuse}), payload (w_{pl}), engine (w_{eng}), and fuel (w_{f}) weights. Assuming the wings retain the same profile shape, the reference area of the wings (S_{ref}) scales proportionally to the weight of the aircraft. At the same time, the weight of the wings scaled proportionally to their reference area. Combining this, an expression for the weight of an aircraft with a modified engine can be obtained as

$$w_{\mathrm{AC}} = \frac{w_{\mathrm{eng}} + w_{\mathrm{fuse}} + w_{\mathrm{f}} + w_{\mathrm{pl}}}{1 - w_{\mathrm{wing,ref}}/w_{\mathrm{AC,ref}}}, \tag{3.12}$$

where variables with the subscript "ref" represent weights from the unmodified aircraft. Aircraft weight is directly proportional to the lift required throughout the flight. To convert lift to drag and eventually to thrust, the lift-drag ratio (L/D) is used. According to Raymer, it can be calculated as

$$L/D|_{\mathrm{max}} = K\sqrt{\frac{\mathrm{AR}}{S_{\mathrm{wet}}/S_{\mathrm{ref}}}}, \tag{3.13}$$

where $K_{L/D}$ is a shape constant, AR is the aspect ratio of the wing, and S_{wet} is the wetted area of the aircraft [41].

The drag caused by the nacelle is proportional to its coefficient of drag. According to Raymer, the drag coefficient of a nacelle ($C_{D,\mathrm{nac}}$) can be expressed as a function of its length (l) and diameter (d) [41], as

$$C_{D,\mathrm{nac}} \propto (1 + 0.35\, d/l)\; l\, d. \tag{3.14}$$

Using these equations, the thrust requirement for an aircraft with a larger and heavier engine can be calculated. As a larger thrust requirement likely necessitates a larger engine, iteration is required to determine the final engine size. As is seen in Section 3.3, proper treatment of installation effects can have a large impact on the results.

Chapter 4

Summary of papers

4.1 Paper 1

As discussed in Chapter 3, the WET engine has been proposed as a candidate for increasing cycle efficiency and decreasing non-CO_2 emissions. However, previous research has had limited treatment of installation effects when evaluating engine performance and has largely restricted the analysis to parameter sweeps. Paper 1 investigates the WET engine performance including installation effects through optimization of cycle and heat exchanger parameters [36]. The engine was evaluated at cruise and take-off conditions and compared to a reference engine.

4.1.1 Methodology

The turbofan simulation code GESTPAN was extended with modules for handling performance calculations of heat exchangers using the GenHEX method, as well as equations for calculating humid combustion. Post processing of the simulation results was developed to take into account the effects of increased engine weight and drag on fuel burn.

First, optimization was performed on 11 parameters, including 5 major cycle parameters and 3 geometric parameters per heat exchanger, with minimum fuel burn as the target. Water-air ratios of up to 50 % was considered. Care was taken to ensure that the engine candidates could provide the required thrust at the most crucial points on a typical mission, while remaining within reasonable temperature limits. Due to the large number of parameters investigated and the sparsity of the feasible design space, optimization was performed using differential evolution, a stochastic optimization routine.

After optimization, the final WET engine design was evaluated and compared to a reference Trent XWB turbofan engine. Parameter sweeps confirmed that an optimal engine design was reached. Additional sweeps were performed on parameters representing improved heat exchanger performance to demonstrate what could potentially be achieved with future technology.

4.1.2 Discussion

The optimized WET engine was shown to have a higher fuel burn than the reference engine for the same payload and mission, with a decrease in specific range of 8.8 %. The cycle efficiency improved by 18 % when adding steam injection. However, pressure losses in the heat exchangers, additional weight, and increased nacelle drag cancel the benefits of the increased efficiency, resulting in a net increase in fuel burn. This result is robust to variations in heat exchanger performance parameters, and future heat exchangers exhibiting near-ideal behavior could at best match the fuel burn of the reference engine.

The optimal turbine inlet temperature (TIT) during cruise was higher than what has previously been suggested. Coupled with the higher specific heat capacity of humid air compared to dry air, this results in substantially higher turbine temperatures and requires cooling further downstream in the turbine stack, complicating engine design and manufacturing. During take-off, substantial amounts of water are required to keep the TIT within feasible limits, while the bypass air is at its highest temperature. The warm bypass air limits the ability of the condenser to collect water, which requires additional water to be drawn from a storage tank.

4.1.3 Division of work

Report writing, heat exchanger modeling and the numerical investigations were performed by Filip Herbertsson. Associate professor Xin Zhao contributed to the modeling of humid combustion. Adjunct professor Anders Lundbladh provided feedback on the report writing. Professor Tomas Grönstedt provided technical supervision for all parts of the work and contributed to the report writing.

4.2 Paper 2

In Paper 2, the total warming impact from all commercial jet airliner flights departing from and arriving at Arlanda during 2025 is analyzed, with a focus on contrails. The paper illustrates the importance of regional aspects for effective contrail mitigation.

4.2.1 Methodology

ADS-B data containing latitude, longitude, and velocity throughout the flights were collected from the OpenSky Network [22] and processed. Aircraft performance was calculated using the Poll-Schumann methodology and emissions were calculated using the Boeing Fuel Flow Method (BFFM2), and the nvPM Mission Emissions Estimation Methodology (MEEM2). The Contrail Cirrus Prediction (CoCiP) model was used to estimate the radiative forcing from contrails. The emissions were combined with forcing response kernels, derived using the Finite Amplitude Impulse Response (FaIR) climate model, to obtain their respective radiative forcing. The climate impact was measured in CO_2 equivalents of energy forcing over 20, 50 and 100 years.

The contrail forcing for the investigated flights was analyzed from a seasonal, temporal, and spatial perspective to determine which factors influence the probability of causing large forcing. The flights were also ranked by their contrail climate impact to determine which individual flights caused the most warming. Additionally, a comparison was made to a previous study focusing on flights in a different region.

4.2.2 Discussion

The results show that contrail forcing is highly unevenly distributed between flights, with the most cooling flight producing a cooling effect 13 times larger than the warming effect from CO_2, and the most warming flight producing a warming effect 57 times larger than that from CO_2. A majority of flights do not produce any contrails at all, and 95 % of the warming effect comes from only 12.1 % of the flights. This shows that, if the right flights are targeted, contrail avoidance could generate a large, cost-effective climate benefit.

The results also show that most contrails are produced during the winter, with forcing in December being 25 times as large as in July. Evening flights also exhibit higher contrail forcing than morning flights. However, the time of day with maximum and minimum forcing depends on whether the flight is departing or arriving and whether it is eastbound or westbound. This shows which flights to focus on when choosing contrail avoidance targets.

The total climate impact is estimated to be 91 % larger than the impact from CO_2 emissions alone when considering a 20-year time horizon, with the largest contributions coming from NO_x, contrails, and stratospheric water vapor. However, the observed contrail forcing was substantially lower than previously reported for North Atlantic flights.

4.2.3 Division of work

Report writing, modeling framework, and the numerical investigations were performed by Filip Herbertsson. Professor Tomas Grönstedt provided technical supervision for all parts of the work and contributed to the report writing.

Chapter 5

Conclusion

5.1 Summary

This thesis investigates the climate impact of aviation with particular emphasis on the role of non-CO_2 emissions and contrail formation, and evaluates potential strategies for mitigating these effects. Key emission sources are characterized and compared using established climate impact metrics, providing a framework for assessing technologies with the potential for substantial environmental improvements and guiding future research priorities.

The climate impact of more than 100,000 Swedish flights is analyzed and attributed to individual emission species. The results reconfirm the importance of non-CO_2 effects and contrails for accurate climate impact assessment, although their relative contribution decreases over longer time horizons. A detailed analysis of contrail impacts reveals strong seasonal, temporal, and spatial variability, with average contrail forcing differing by up to a factor of 25 between winter and summer. Furthermore, approximately 12% of flights are responsible for the majority of contrail-induced warming. These findings highlight the potential effectiveness of targeted mitigation strategies, such as selective contrail avoidance.

In addition, the Water Enhanced Turbofan (WET) engine is evaluated as a candidate technology for reducing both CO_2 and non-CO_2 emissions, as well as contrail formation. Its fuel burn performance is assessed using state-of-the-art conceptual heat exchanger modeling and feasibility analysis under thermodynamic constraints. The results indicate that installation effects are likely to outweigh efficiency gains, leading to increased fuel burn compared to a modern reference engine [36]. This outcome is robust across variations in heat exchanger performance, limiting the potential for future improvements. Furthermore, the cycle is inherently challenged by an increased turbine exhaust temperature. This necessitates additional system components, such as a water storage tank and low-pressure turbine cooling, increasing overall design complexity.

5.2 Future work

Future work should build on the identification of high-impact flights by evaluating the feasibility and effectiveness of targeted contrail avoidance strategies. This includes quantifying the potential climate benefits of such measures while accounting for operational constraints, such as airspace structure, air traffic management, and fuel penalties, to ensure that proposed mitigation strategies are practically implementable.

Given the complexity of real-world aviation operations, purely theoretical assessments are unlikely to capture all relevant factors. Collaboration with industry stakeholders, such as airlines and air navigation service providers, would therefore be valuable for experimentally testing and validating the most promising mitigation strategies. Such efforts would provide critical evidence on the operational feasibility of contrail avoidance and support decision-making by regulators and other stakeholders aiming to reduce aviation's climate impact.

Regarding propulsion technologies, the present analysis identifies the condenser as a key limitation to the efficiency and feasibility of the WET engine, due to its size, weight, and dependence on low ambient temperatures for effective condensation. Future research should investigate proposed cycle modifications aimed at improving condensation performance and reducing system complexity [10]. In addition, alternative concepts involving water injection and recuperation, such as HySIITE, warrant further study, as they may avoid some of the thermodynamic constraints identified for the WET engine and offer improved fuel efficiency. Applying a consistent evaluation methodology to these concepts would enable a more robust comparison of their potential climate benefits.

Bibliography

[1] Volker Grewe et al. "Evaluating the climate impact of aviation emission scenarios towards the Paris agreement including COVID-19 effects". In: *Nature Communications* 12.1 (June 2021). ISSN: 2041-1723. DOI: `10.1038/s41467-021-24091-y` (cit. on pp. 3, 4).

[2] D. S. Lee et al. "Transport impacts on atmosphere and climate: Aviation". In: *Atmospheric Environ.* 44 (2010), pp. 4678–4734. DOI: `10.1016/j.atmosenv.2009.06.005` (cit. on p. 3).

[3] Anastasia Kharina and Daniel Rutherford. *Fuel efficiency trends for new commercial jet aircraft: 1960 to 2014*. (accessed: 2026-05-04). 2015. URL: `https://trid.trb.org/View/1372314` (cit. on p. 3).

[4] Airbus. *Global Market Forecast 2018-2037*. Global Networks, Global Citizens, 2018. ISBN: 978-2-9554382-3-6 (cit. on p. 3).

[5] Boeing. *Commercial Market Outlook 2019–2038*. 2019 (cit. on p. 3).

[6] D.S. Lee et al. "The contribution of global aviation to anthropogenic climate forcing for 2000 to 2018". In: *Atmospheric Environment* 244 (Jan. 2021), p. 117834. ISSN: 1352-2310. DOI: `10.1016/j.atmosenv.2020.117834` (cit. on pp. 4, 5, 8, 15, 16).

[7] Mafalda Narciso and João M. Melo de Sousa. "Influence of Sustainable Aviation Fuels on the Formation of Contrails and Their Properties". In: *Energies* 14.17 (Sept. 2021), p. 5557. ISSN: 1996-1073. DOI: `10.3390/en14175557` (cit. on p. 9).

[8] Christiane Voigt et al. "Cleaner burning aviation fuels can reduce contrail cloudiness". In: *Communications Earth & Environment* 2.1 (June 2021). ISSN: 2662-4435. DOI: `10.1038/s43247-021-00174-y` (cit. on p. 10).

[9] Eytan J. Adler and Joaquim R. R. A. Martins. "Blended Wing Body Configuration for Hydrogen-Powered Aviation". In: *Journal of Aircraft* 61.3 (May 2024), 887–901. ISSN: 1533-3868. DOI: `10.2514/1.c037582` (cit. on p. 10).

[10] Antonio Bruno de Vasconcelos Leitão, Cleverson Bringhenti, Jesuino Takachi Tomita, Franco Jefferds dos Santos Silva, Carlos Xisto, and Tomas Grönstedt. "A review of hydrogen aircraft propulsion systems: recent advances and environmental perspectives". In: *International Journal of Hydrogen Energy* 176 (Oct. 2025), p. 151489. ISSN: 0360-3199. DOI: `10.1016/j.ijhydene.2025.151489` (cit. on pp. 10, 36).

[11] Susanne Pettersson, Christian Azar, and Daniel Johansson. “Climate impact of contrail cirrus from hydrogen combustion aircraft”. In: *EGUsphere* (Sept. 2025). DOI: 10.5194/egusphere-2025-3535 (cit. on p. 10).

[12] Christiane Voigt et al. “Substantial aircraft contrail formation at low soot emission levels”. In: *Nature* 652.8108 (Apr. 2026), 112–118. ISSN: 1476-4687. DOI: 10.1038/s41586-026-10286-0 (cit. on p. 10).

[13] O. Schmitz, H. Klingels, and P. Kufner. “Aero Engine Concepts Beyond 2030: Part 1—The Steam Injecting and Recovering Aero Engine”. In: *J. of Eng. for Gas Turbines and Power* 143.2 (2021), p. 021001. DOI: https://doi.org/10.1115/1.4048985 (cit. on pp. 10, 21, 25).

[14] Ernst Schmidt. “Die entstehung von eisnebel aus den auspuffgasen von flugmotoren”. In: *Schriften der Deutschen Akademie der Luftfahrtforschung, Verlag R. Oldenbourg, München, Heft 44* 5.44 (1941), pp. 1–15 (cit. on p. 14).

[15] Herbert Appleman. “The formation of exhaust condensation trails by jet aircraft”. In: *Bulletin of the American Meteorological Society* 34.1 (1953), pp. 14–20 (cit. on p. 14).

[16] U. Schumann. “A contrail cirrus prediction model”. In: *Geoscientific Model Development* 5.3 (May 2012), 543–580. ISSN: 1991-9603. DOI: 10.5194/gmd-5-543-2012 (cit. on p. 16).

[17] U. Schumann, B. Mayer, K. Graf, and H. Mannstein. “A Parametric Radiative Forcing Model for Contrail Cirrus”. In: *Journal of Applied Meteorology and Climatology* 51.7 (July 2012), 1391–1406. ISSN: 1558-8432. DOI: 10.1175/jamc-d-11-0242.1 (cit. on p. 16).

[18] Ulrich Schumann et al. “Properties of individual contrails: a compilation of observations and some comparisons”. In: *Atmospheric Chemistry and Physics* 17.1 (Jan. 2017), 403–438. ISSN: 1680-7324. DOI: 10.5194/acp-17-403-2017 (cit. on p. 16).

[19] Roger Teoh, Ulrich Schumann, Arnab Majumdar, and Marc E. J. Stettler. “Mitigating the Climate Forcing of Aircraft Contrails by Small-Scale Diversions and Technology Adoption”. In: *Environmental Science & Technology* 54.5 (Feb. 2020), 2941–2950. ISSN: 1520-5851. DOI: 10.1021/acs.est.9b05608 (cit. on p. 16).

[20] Roger Teoh, Ulrich Schumann, Edward Gryspeerdt, Marc Shapiro, Jarlath Molloy, George Koudis, Christiane Voigt, and Marc E. J. Stettler. “Aviation contrail climate effects in the North Atlantic from 2016 to 2021”. In: *Atmospheric Chemistry and Physics* 22.16 (Aug. 2022), 10919–10935. ISSN: 1680-7324. DOI: 10.5194/acp-22-10919-2022 (cit. on p. 16).

[21] Roger Teoh, Ulrich Schumann, Christiane Voigt, Tobias Schripp, Marc Shapiro, Zebediah Engberg, Jarlath Molloy, George Koudis, and Marc E. J. Stettler. “Targeted Use of Sustainable Aviation Fuel to Maximize Climate Benefits”. In: *Environmental Science & Technology* 56.23 (Nov. 2022), 17246–17255. ISSN: 1520-5851. DOI: 10.1021/acs.est.2c05781 (cit. on p. 16).

[22] M Schäfer, M Strohmeier, V Lenders, I Martinovic, and M Wilhelm. "Bringing up OpenSky: A large-scale ADS-B sensor network for research". In: *ACM/IEEE International Conference on Information Processing in Sensor Networks* (2014) (cit. on pp. 16, 32).

[23] Angela Nuic. "User manual for the Base of Aircraft Data (BADA) revision 3.10". In: *Atmosphere* 2010 (2010), p. 001 (cit. on p. 17).

[24] DIA Poll and Ulrich Schumann. "An estimation method for the fuel burn and other performance characteristics of civil transport aircraft in the cruise. Part 1 fundamental quantities and governing relations for a general atmosphere". In: *The Aeronautical Journal* 125.1284 (2021), pp. 257–295. DOI: 10.1017/aer.2020.62 (cit. on p. 17).

[25] DIA Poll and Ulrich Schumann. "An estimation method for the fuel burn and other performance characteristics of civil transport aircraft during cruise: part 2, determining the aircraft's characteristic parameters". In: *The Aeronautical Journal* 125.1284 (2021), pp. 296–340. DOI: 10.1017/aer.2020.124 (cit. on p. 17).

[26] Gabriel Jarry, Daniel Delahaye, and Christophe Hurter. "Towards aircraft generic Quick Access Recorder fuel flow regression models for ADS-B data". In: *International Conference on Research in Air Transportation.* (accessed 17 March 2026). 2024 (cit. on p. 17).

[27] Fangqun Yu, Bernd Karcher, and Bruce E Anderson. "Revisiting contrail ice formation: Impact of primary soot particle sizes and contribution of volatile particles". In: *Environmental science & technology* 58.40 (2024), pp. 17650–17660. DOI: 10.1021/acs.est.4c04340 (cit. on p. 18).

[28] Denise Ahrens, Yoann Méry, Adrien Guénard, and Richard C Miake-Lye. "A new approach to estimate particulate matter emissions from ground certification data: The nvPM mission emissions estimation methodology". In: *Journal of Engineering for Gas Turbines and Power* 145.3 (2023), p. 031019. DOI: 10.1115/1.4055477 (cit. on p. 18).

[29] Denise Ahrens, Brian Kim, Yoann Méry, Joseph Zelina, Rudolph Dudebout, and Richard C Miake-Lye. *The Aircraft nvPM Mission Emissions Estimation Methodology, Version 2 (MEEM2).* Tech. rep. SAE Technical Paper, 2025. DOI: 10.4271/2025-01-6000 (cit. on p. 18).

[30] Gaby Rädel and Keith P. Shine. "Validating ECMWF forecasts for the occurrence of ice supersaturation using visual observations of persistent contrails and radiosonde measurements over England". In: *Quarterly Journal of the Royal Meteorological Society* 136.652 (2010), 1723–1732. ISSN: 0035-9009. DOI: 10.1002/qj.670 (cit. on p. 19).

[31] A Martin Frias, M L Shapiro, Z Engberg, R Zopp, M Soler, and M E J Stettler. "Feasibility of contrail avoidance in a commercial flight planning system: an operational analysis". In: *Environmental Research: Infrastructure and Sustainability* 4.1 (Mar. 2024), p. 015013. ISSN: 2634-4505. DOI: 10.1088/2634-4505/ad310c (cit. on p. 20).

[32] Banavar Sridhar, Neil Y Chen, and Hok K Ng. “Energy efficient contrail mitigation strategies for reducing the environmental impact of aviation”. In: *Tenth USA/Europe Air Traffic Management Research and Development Seminar (ATM2013)*. 2013 (cit. on p. 20).

[33] S. Kaiser, O. Schmitz, and H. Klingels. “Aero Engine Concepts Beyond 2030: Part 2 — The Free-Piston Composite Cycle Engine”. In: *Turbo Expo: Power for Land, Sea, and Air*. Vol. 5. 2020, V005T06A018. DOI: `https://doi.org/10.1115/GT2020-15395` (cit. on p. 21).

[34] O. Schmitz et al. “Aero Engine Concepts Beyond 2030: Part 3—Experimental Demonstration of Technological Feasibility”. In: *J. of Eng. for Gas Turbines and Power* 143.2 (2021), p. 021003. DOI: `https://doi.org/10.1115/1.4048994` (cit. on p. 21).

[35] D. Y. Cheng. “Parallel-compound dual-fluid heat engine”. Pat. US Patent 3,978,661. 1976 (cit. on p. 21).

[36] Filip Herbertsson, Xin Zhao, Anders Lundbladh, and Tomas Grönstedt. “Performance assessment of the Water Enhanced Turbofan engine”. In: *Aerospace Science and Technology* 178 (Nov. 2026), p. 112389. ISSN: 1270-9638. DOI: `10.1016/j.ast.2026.112389` (cit. on pp. 23, 24, 26, 31, 35).

[37] Sascha Kaiser, Oliver Schmitz, Paul Ziegler, and Hermann Klingels. “The Water-Enhanced Turbofan as Enabler for Climate-Neutral Aviation”. In: *Applied Sciences* 12.23 (Dec. 2022), p. 12431. ISSN: 2076-3417. DOI: `10.3390/app122312431` (cit. on pp. 25, 26).

[38] S Larry Dixon and Cesare Hall. *Fluid mechanics and thermodynamics of turbomachinery*. Butterworth-Heinemann, 2013 (cit. on p. 27).

[39] T. Grönstedt. “Development of methods for analysis and optimization of complex jet engine systems”. PhD thesis. Chalmers University of Technology, 2000 (cit. on p. 28).

[40] Petter Miltén, Isak Johnsson, Anders Lundbladh, and Carlos Xisto. “Generalized Method for the Conceptual Design of Compact Heat Exchangers”. In: *Journal of Engineering for Gas Turbines and Power* 146.11 (Aug. 2024). ISSN: 1528-8919. DOI: `10.1115/1.4065922` (cit. on p. 28).

[41] D. P. Raymer. *Aircraft Design: A Conceptual Approach*. 6th ed. Reston, VA: American Institute of Aeronautics and Astronautics, 2018 (cit. on p. 29).